Mutations in the M4 Domain of the *Torpedo californica* Nicotinic Acetylcholine Receptor Alter Channel Opening and Closing

S.I. Ortiz-Miranda[1], J.A. Lasalde[2,*], P.A. Pappone[1], M.G. McNamee[2]

[1]Section of Neurobiology, Physiology and Behavior, Division of Biological Sciences, University of California, Davis, CA 95616, USA
[2]Section of Molecular and Cellular Biology, Division of Biological Sciences, University of California, Davis, CA 95616 USA

Abstract. We studied the functional effects of single amino acid substitutions in the postulated M4 transmembrane domains of *Torpedo californica* nicotinic acetylcholine receptors (nAChRs) expressed in *Xenopus* oocytes at the single-channel level. At low ACh concentrations and cold temperatures, the replacement of wild-type α418Cys residues with the large, hydrophobic amino acids tryptophan or phenylalanine increased mean open times 26-fold and 3-fold, respectively. The mutation of a homologous cysteine in the β subunit (β447Trp) had similar but smaller effects on mean open time. Coexpression of α418Trp and β447Trp had the largest effect on channel open time, increasing mean open time 58-fold. No changes in conductance or ion selectivity were detected for any of the single subunit amino acid substitutions tested. However, the coexpression of the α418Trp and β447Trp mutated subunits also produced channels with at least two additional conductance levels. Block by acetylcholine was apparent in the current records from α418Trp mutants. Burst analysis of the α418Trp mutations showed an increase in the channel open probability, due to a decrease in the apparent channel closing rate and a probable increase in the effective opening rate. Our results show that modifications in the primary structure of the α- and β subunit M4 domain, which are postulated to be at the lipid-protein interface, can significantly alter channel gating, and that mutations in multiple subunits act additively to increase channel open time.

Key words: *Torpedo californica* — Site-directed mutagenesis — Single-channel electrophysiology — Ion channel gating — Burst analysis

Introduction

The nicotinic acetylcholine receptor (nAChR) has been extensively studied using biochemical, pharmacological, biophysical and molecular genetic techniques, making it one of the best characterized of the physiologically important ion channels (for reviews *see* Ochoa, Chattopadhyay & McNamee, 1989; Galzi et al., 1991; Changeux et al., 1992; Pradier & McNamee, 1992; Unwin, 1993; Karlin & Akabas, 1995). Although the primary structures of the channels from many different species have been known for many years (*see* Changeux et al., 1992), it is not yet possible to predict the relationships among the chemical, structural and functional features of the channel with confidence. Indirect approaches must still be used to understand how structural areas of the channel determine its ion transporting and kinetic properties.

Nicotinic acetylcholine receptors are complex postsynaptic transmembrane glycoproteins formed by homologous subunits arranged around an axial channel pore. In tissues like the *Torpedo californica* fish electric organ and mammalian skeletal muscle, the receptor's four subunits are assembled in a stoichiometry of $(\alpha)_2\beta\gamma$(or ϵ)δ. In most neuronal tissues the nAChR is composed of only one or two distinct subunits believed to be arranged in a pentameric structure with a stoichiometry $(\alpha)_5$ or $(\alpha)_2$ $(\beta)_3$ (Cooper, Couturier & Ballivet, 1991; Anand et al., 1991). Hydropathy profiles of the protein sequences reveal that each of the receptor subunits has four homologous but topographically distinct transmembrane domains, called M1, M2, M3 and M4 (Noda et al., 1983; Devillers-Thiery et al., 1983).

---

* *Present address:* Department of Biology, University of Puerto Rico, San Juan, PR 00931

Correspondence to: M.G. McNamee

MUSCLE-TYPE AChR:

                                    ↓
```
Torpedo   α   ILLCVFMLICIIGTVSVFA
Calf      α   ILLAVFMLVCIIGTLAVFA
Chicken   α   LLLVIFMLVCIIGTLAVFA
Human     α   ILLGVFMLVCIIGTLAVFA
Xenopus   α   ILLAVFMTVCVIGTLAVFA
Mouse     α   ILLGVFMLVCLIGTLAVFA


Torpedo   β   LFLYVFFVICSIGTFSIFL
Calf      β   LFLWTFIIFTSVGTLVIFL
Mouse     β   LFLWTFIVFTSVGTLVIFL
```

NEURONAL AChR:

```
Chicken   α2   IFLWMFIIVCLLGTVGLFA
Chicken   α3   IFLWVFILVCILGTAGLFL
Chicken   α4   IFLWMFIIVCLLGTVGLFL
Chicken   α5   MFLWAFLLVSIIGSLVLFI
Chicken   α7   LCLMAFSVFTIICTIGILM
Chichen   α8   LCLVAFTLFAIICTFTILM


Rat       α2   IFLWLFIIVCFLGTIGLFL
Rat       α3   IFLWVFILVCILGTAGLFL
Rat       α4   IFLWMFIIVCLLGTVGLFL
Rat       α5   MFLWTFLLVSIIGTLGLFV
Rat       α6   VFLWVFIIVCVFGTVGLFL
Rat       α7   MAFSVFTIICTIGILMSAP
```

Fig. 1. Amino acid sequences of the M4 transmembrane domain of neuronal α subunit and muscle-type α and β subunits of the nAChR. Bold letters indicate residues that are conserved across different tissues and species. Arrow indicates the *Torpedo* α418Cys position within the M4 amino acid sequence.

Selective chemical modification of purified nAChR from fish electric organs has been used over the past twenty years to probe structure-function relationships. Photoaffinity labeling and mutagenesis experiments point strongly toward an M2 contribution to the walls of the ion channel (Hucho, Oberthur & Lottspeich, 1986; Imoto et al., 1986, 1988; Giraudat et al., 1989). The specific functions of the other hydrophobic domains are not as well-characterized, although there is evidence based on chemical labeling studies to indicate that M4 is located at the protein-lipid interface of the membrane (Giraudat et al., 1985; Blanton & Cohen, 1992). Recent work on lipid composition and anesthetic effects has shown that the protein-lipid interface of the nAChR channel is more sensitive than expected to perturbations in the receptor environment, which can lead to substantial alterations in channel activity (Earnest et al., 1986; Fong & McNamee, 1986, 1987; Sunshine & McNamee, 1992, 1994).

Several previous modification studies have focused

on cysteine residues since free sulfhydryl groups have been shown in chemical modification studies to have a significant functional role in receptor activity (Yee, Corley & McNamee, 1986; Clarke & Martinez-Carrion, 1986; Walker, Richardson & McNamee, 1984; Kao et al., 1984; Huganir & Racker, 1982). Site-directed mutagenesis (Li et al., 1990) showed that mutations at γ451Cys to Phe or Ser in the M4 domain substantially inhibited the channel activity as measured from voltage clamp whole cell currents in *Xenopus laevis* oocytes expressing *Torpedo* nAChR. There are six amino acid positions within the M4 domain of the α subunit that are evolutionarily very conserved among different tissues and species as shown in Fig. 1. Mutation of α418Cys to Trp produced a dramatic increase in the macroscopic current response to acetylcholine (ACh) (Li et al., 1992). A series of amino acid substitutions at this position and at the homologous 447Cys of the β subunit were examined in an effort to correlate channel activity with a particular structural property conferred by the substituted amino acids (Lee et al., 1994). Some of the mutations increased the ACh-induced macroscopic currents and their desensitization rates and increased channel mean open times. Based on that study, a kinetic model was proposed in which decreased channel closing rates were sufficient to explain the increases in mutant nAChR macroscopic currents. In the present work, we extend our previous analysis of the αC418 M4 position (Lee et al., 1994) to include an equivalent position of the β subunit and we present a more detailed characterization of these mutations using single-channel analysis. Changes in the mean open time and steady-state open probability (P_0), mainly due to changes in the channel effective closing rates and/or possible changes in channel opening and binding rates, are interpreted in terms of allosteric interactions linking the lipid-protein interface with the ion channel domain of the receptor.

Materials and Methods

RECOMBINANT DNA MANIPULATIONS

Site-directed mutagenesis was carried out following the procedure described by Lee et al. (1994). In general, point mutations were generated by mismatch amplification using two sequential polymerase chain reactions (PCR) (Horton & Pease, 1991). These mutagenic fragments were fused to generate a single fragment containing the mutation and then amplified a second time by PCR reaction. Once the mutagenic fragments were purified, they were digested at unique restriction sites with specific nucleases (in our case BgII & EcoRI) able to generate complementary ends in the fragment as well as in the plasmid (pGEM3Z(−)) (Promega, Madison, WI) used as the vector. After the plasmid and the mutagenic fragment were ligated with T4 ligase, competent αDH5 *E. coli* cells were transformed. The transformed cells were grown in agar plates containing 100 μg/ml of ampicillin for 24 hr. DNA from the colonies was used to sequence the whole plasmid insert

to insure that the desired mutation was present and no other changes had occurred (Sequenase, Version 2.0, United States Biochemical, Cleveland, OH).

RNA Transcription and Expression into *X. laevis* Oocytes

DNA from the transformed *E. coli* cells was used to generate RNA transcripts by *in vitro* transcription using SP6 polymerase (Lee et al., 1994). The transcripts of the mutated subunit were purified and then mixed with RNA transcripts for the other nAChR subunits (*see* Pradier, Yee & McNamee, 1989 for a description of the cDNA templates used) in a ratio of $2 \times \alpha$, $1 \times \beta$, $1 \times \gamma$, $1 \times \delta$. For the coexpression of α418Trp/β447Trp, mRNA coding for both mutated subunits was mixed in the same ratio as described. Fifty nanoliters (at a concentration of 1 ng/nl) of the mRNA mixture was microinjected into stage V and VI oocytes that had been extracted, cleaned and defolliculated in Ca^{++}-free OR2 buffer (Wallace et al., 1973) by collagenase (Type 1A, Sigma, St. Louis, MO) and manual dissection. Oocytes were kept at 18°C in L-15 media (Gibco, Gaithersburg, MD) supplemented with 0.4% BSA and $1\times$ antibiotic-antimycotic solution (cat# 600-5245AE, Gibco). They were used between day 3 and day 6 after injection. Apart from the common variations from patch-to-patch, no significant differences in single channel characteristics were seen within any channel type.

Electrophysiology

Oocytes expressing the *Torpedo californica* AChR were transferred to a hypertonic solution composed of (in mM): 150 NaCl, 2 KCl, 5 HEPES and 3% (w/v) sucrose (pH 7.6) for 15 to 30 min to allow them to shrink. The vitelline membrane was removed manually and the oocytes were transferred to the recording chamber and washed with 5 to 10 volumes of a bath solution consisting of (in mM): 100 KCl, 1 $MgCl_2$, 10 HEPES (pH 7.2). Single-channel currents were recorded at 10 KHz using the patch-clamp techniques described by Hamill et al. (1981) in the on-cell and outside-out configurations using a L/M-EPC 7 patch-clamp amplifier interfaced by a Cheshire Data Interface to a DEC LSI 11/73 computer system (INDEC Systems, Sunnyvale, CA) or a Dagan 3900 amplifier interfaced by a TL-1 DMA (Axon Instruments, Foster City, CA) to an IBM-compatible computer. Patch pipettes were made of thick-walled borosilicate glass (Sutter Instruments, Novato, CA) displaying resistances of 6 to 11 MΩ. The pipette (external) solution was composed of (in mM): 100 KCl, 10 HEPES, 10 EGTA (pH 7.2) and 1 to 50 μM ACh. Following the gigaohm seal formation (>10 GΩ), the chamber was cooled to a desired temperature by adjusting the flow of an iced water circulation line enclosing the recording bath chamber. The temperature was monitored with a thermocouple (400 Series Probe, YSI, Yellow Springs, OH) placed inside the bath chamber. All the temperatures reported here have an error of ±1°C. The data generated in this way were recorded on VHS tapes for later analysis using a modified digital audio processor (VR-10B and VR-10C, Instrutech, Mineola, NY).

Analysis

With the exception of burst analysis, pCLAMP software (AXON Instruments) was used for the construction and the statistical analysis of the data files. The data traces were played back, low-pass filtered at 4 to 20 kHz using an 8-pole Bessel filter (Frequency Devices, Haverhill, MA) and digitized at rates varying from 20 μs to 100 μs depending on the mutation being tested and the temperature used during the experiment. The data reduction step was performed using the IPROC3 software programs (Sachs, Neil & Barkakati, 1982) also distributed by Axon Instruments. Mean amplitude values were used in establishing a window of detection for each file so that all the events falling within the mean plus or minus a variable amplitude were accepted and added into a list of events that was then tested statistically using the pCLAMP software. The window limits were in general 1 pA above and below the mean amplitude value but they were modified when other channels were present in the patch in order to exclude them from the analysis. To study subconductance levels, a wide window including all channel amplitudes was used initially. The different levels were differentiated using an amplitude distribution histogram and reanalyzed using a narrower window able to discriminate between them. The mean open time values reported in the Table for the α418Trp/β447Trp mutants were obtained by setting the window of detection to accept only the major conductance levels. Although the changes in conductance within the same channel opening were not frequent, they were present occasionally, so some transitions to the small 40 pS subconductance level were treated as closings. The mean open time reported is then a conservative one, probably smaller than the value that could be obtained if all subconductance values were accepted within the same opening.

For burst analysis, the list of events generated by IPROC3 was analyzed using LPROC software (Neil, Xiang & Auerbach, 1991). A homogeneous list of bursts was created with this program, as described below, and fitted statistically to calculate mean open times, closed times, and rate constants. The term burst will be used indiscriminately in this paper to refer to groups of channel openings at low as well as at higher ACh concentrations, even though they describe different mechanisms in terms of channel opening (Sakmann et al., 1980; Colquhoun & Sakmann, 1981; Colquhoun & Hawkes, 1981).

Closed intervals within the record were fitted by the sum of two to five exponentials, depending on the ACh concentration. At low concentrations, the fast component was assumed to reflect reopenings of singly or doubly-liganded channels, and the slow component was assumed to represent periods between activations of different channels. For ACh concentrations $\geq$10 μM bursts were defined by a burst terminator (BTERM), a time 3 to 5 times longer than the slowest maximum time a channel stays closed while it is bursting. This closed time duration is normally represented by the presence of a slower component that accounts for more than 70% of the total closed intervals in the record. Setting the burst terminator factor (BTERM) to be 3 to 5 times this value (normally around 3.5 in our case) allowed us to include around 95 to 99% of all the intraburst closures in the kinetic analysis (Auerbach & Lingle, 1986). Once BTERM was established, a list of bursts was generated and a subset of bursts was selected for further analysis. The purpose of burst selection is to eliminate the contribution of currents from dissimilar conductance and uncommon kinetic forms of AChR. Bursts were selected based on several criteria, including the mean open channel current amplitude, mean open interval duration, and probability of being open. The ranges used for each of these parameters were determined after examining the means and variances for bursts in the entire record. The minimum number of openings within the bursts was set to 4 to reduce the scatter in open probabilities (P_o). Once a subset of bursts was finally selected, a list of the durations of open and closed intervals within those bursts was made and their respective distributions fitted by a nonlinear least squares algorithm in which the integral of the exponential probability density function was evaluated over each bin (for details *see* Sachs & Auerbach, 1983).

Because at intermediate concentrations of ACh the identification of the different closed time components is difficult, we made use of P_os and the channel closing rates (α_1 and α_2) to corroborate the identity of the components being analyzed. Even though P_o values can be the product of the two possible activation pathways, only P_os and α_2 values
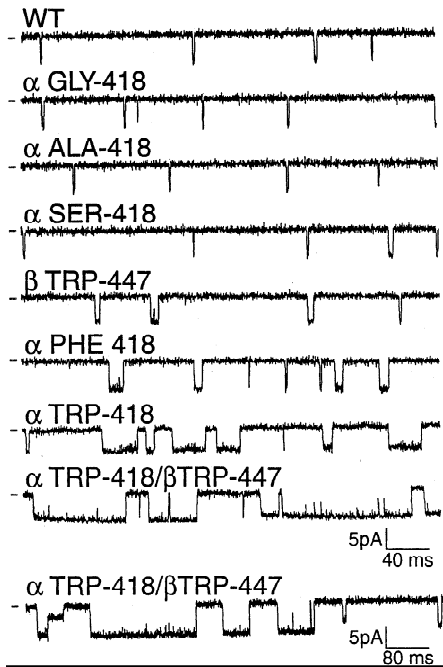
Fig. 2. Single-channel currents from all mutations recorded from on-cell patches. Openings are downward deflections, zero current level is denoted by the horizontal dash. The bottom record shows the three subconductance levels detected in some of the patches expressing the α418Trp/β447Trp mutant. The holding potential was −80 mV, 4 μM ACh. The bath temperature was 13 ± 1°C for all records with the exception of α418Ala (16°C) and α418Trp/β447Trp (21°C). Sampled at 100 μsec and filtered at 4–5 kHz.

showed effective opening rates (β′) values close to the ones shown by the major slow components in the closed-time distributions.

Some patches were also analyzed with pCLAMP6 software (Axon Instruments). Open and closed time duration distributions were constructed from the IPROC3 generated files and fitted by a Marquardt or simplex least squares routine in PSTAT. The relative areas for each component were calculated as a function of the number of events forming each component.

To estimate EC_{50}s, Hill coefficients, or maximum values from the different dose-response curves, we used the Hill equation:

$$Y = B/[1 + (k[A])^H] \tag{1}$$

where Y is the response value (i.e., P_o) calculated at a particular concentration of agonist A; B is the maximum value reached during saturation; k is the agonist concentration at which $Y = B/2$ (EC_{50}); and H is the Hill coefficient.

A single open-closed kinetic model was assumed when the apparent open and closed time constants were corrected for missed events (Colquhoun & Sigworth, 1983) although this model does not describe our data in full. The duration of the minimum detected event was 20 μsec. Since our apparent mean open times are much larger than the minimum detected events, we are assuming that most of the openings are detected and only the fast closures (or gaps) within an opening were missed (Colquhoun & Sigworth, 1983). For the mean open time corrections we used the corrected mean closed time values belonging to the fastest component in the closed time distributions.

Results

CHANNEL OPEN TIME

Representative single-channel currents recorded from cell-attached patches on *Xenopus laevis* oocytes expressing WT or mutant *Torpedo californica* nAChRs at position 418 on the α subunit or the homologous 447 position on the β subunit are shown in Fig. 2. Continuous records from each patch, recorded between day 3 and 4 after mRNA injection, are shown in the presence of 4 μM ACh at a potential of −80 mV. This ACh concentration was low enough to avoid a deep desensitization of the channel, but high enough to have a sizable population of openings to study. In previous two-microelectrode voltage-clamp studies, this concentration was able to induce ~8% of the maximal current in oocytes expressing WT channels and ~14% in those expressing α418Trp (Lee et al., 1994). Mutations of the α418 Cys to Gly, Ala, or Ser had no obvious effects on single channel currents, but substantial increases in open time are clearly seen for the Phe and Trp mutations.

Open time distributions for all the AChRs examined showed two components (*see* Fig. 5). Exponential fits of the open times indicate that changes from the WT cysteine to small, nonpolar amino acids like α418Gly and α418Ala or to the more polar small amino acid serine had no significant effect on either of the fast and slow open time components. However, replacing cysteine with large aromatic amino acids in the β447Trp, α418Phe, α418Trp and α418Trp/β447Trp mutants (*see* Fig. 3) greatly increased the slow component open time ($\tau_{o,2}$), while the fast open time component $\tau_{o,1}$ remains unchanged (*see* Fig. 5*A* and *B*, left panels). The fast component was recorded at our system resolution limit so there is the possibility that the absence of differences between mutants and/or WT channels might be a product of our recording limitations. Furthermore, it was particularly hard to separate the components at high ACh concentrations. The Table shows mean open time values from the slower open component ($\tau_{o,2}$) for all the receptor types examined. These open times were longer for all the Cys → Trp mutants, and increased in duration when more subunits carried the mutation. Assuming equivalence between both α-subunits, these changes in mean open times corresponded to comparable increments in free energy for the closing transition with increments in the number of mutated subunits in the receptor. Thus, the single subunit substitution, β447Trp, increased $\tau_{o,2}$ twofold ($\Delta U = 0.39$ kcal/mol), the double subunit α418Trp mutation increased $\tau_{o,2}$ 26-fold ($\Delta U = 1.86$ kcal/mol), and the coexpression of α418Trp and β447Trp mutants showed the largest change in open time, increasing $\tau_{o,2}$ 58-fold ($\Delta U = 2.31$ kcal/mol) compared to WT. Substitution with the smaller aromatic amino acid phenylalanine at α418 had qualitatively simi-
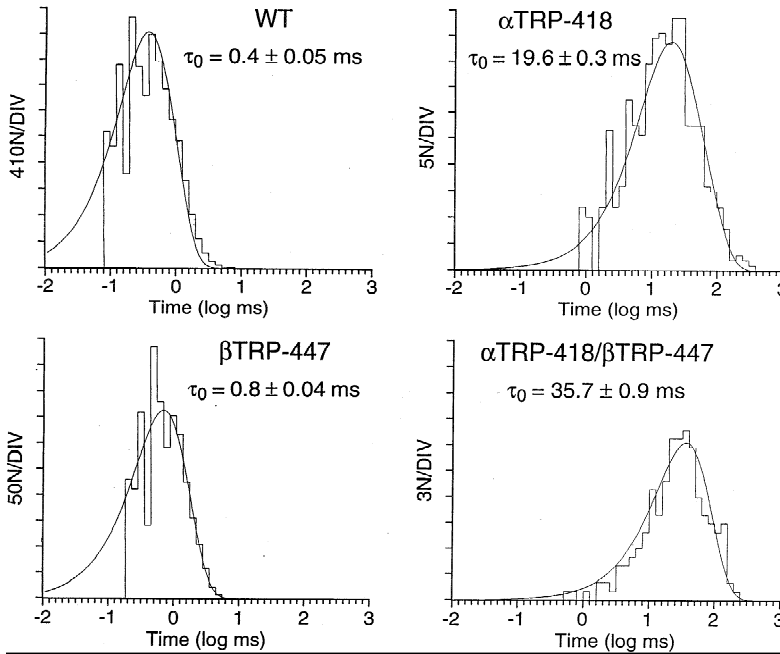
Fig. 3. Mutations alter channel open time. Mean open time distributions for all the receptor types containing tryptophan substitutions showing the slower open time component $\tau_{o,2}$ only. The distributions were constructed from single cell-attached patches for WT (36095 events), β447Trp (3417 events), and α418Trp/β447Trp (207 events). Two patches from the same oocyte were used to construct the distribution of α418Trp (574 events). Recording conditions were: potential −100 mV; temperature 14°C; ACh 4 μM except for α418Trp, which was 1 μM. Sampling was set to 50 μsec for WT and β447Trp; 100 μsec for α418Trp and α418Trp/β447Trp.

lar but lesser effects than Trp on open time. Thus, hydrophobicity, and size of the substituted residue and number of substitutions per receptor appear to be salient determinants in the mutation effects on open time.

No significant differences were detected between WT and mutant channels in the Q_{10} for slow open time component measured between 12° and 22°C, as shown in the Table. The Q_{10} values for mean open time (3.3 to 3.8) are higher than reported for on-cell patches (2.1 to 2.9) in BC3H-1 cells (Dilger et al., 1991) and are similar to the values for outside-out patches in the same report (3.0 to 4.2). However, our estimation of the temperature dependence of mean open times is around 4 times smaller than reported by Sine et al. (1990) for *Torpedo* channels expressed in fibroblasts. Differences in expression systems may account for the discrepancies between Q_{10} values. Recently, Zanello et al. (1996) found that mouse AChR expressed in different cell lines showed noticeable differences in channel closing rates. The difference was postulated to be the result of receptor exposition to dissimilar cell membrane environments.

CHANNEL CLOSED TIMES

To determine whether the α418Trp substitution also affects channel opening kinetics, bursts of channel openings were analyzed and mutant channels compared to WT. The burst analysis allows the estimation of channel closed times, based on the assumption that each burst represents a single channel that is oscillating between open and closed states (Sakmann, Patlak & Neher, 1980). The temperature for these experiments was 18 ± 1°C to increase overall channel activity. Different concentra-

tions of ACh were used, ranging from 4 μM to 100 μM for the WT channels, and from 4 μM to 50 μM for the α418Trp mutant. Bursts were more difficult to study at both ends of the concentration range because of desensitization and channel block by ACh, or extremely low channel activity.

Figure 4A shows the bursting behavior expressed by WT and α418Trp channels on a slow time scale. Figure 4B shows records of individual bursts at three different ACh concentrations for WT (left) and α418Trp (right). Note that qualitatively the durations of the closed intervals within the bursts are reduced as the ACh concentration was increased in both channel types. Also the duration of the open intervals within the burst in the α418Trp mutant decreased with increasing ACh concentrations, probably because of channel flickering behavior induced by agonist block. This behavior can be seen quantitatively in the open and closed time distributions presented in Fig. 5 for both WT and mutant channels. Figure 5A and B (left panels) show the mean open time distributions for both receptor types at 4 μM and 50 μM, respectively. Changes in mean closed times and their respective areas can be seen in Figure 5A and B (right panels) between both receptor types. Those changes and their interpretation in terms of a kinetic scheme are discussed below. The following sequential scheme is used to describe the channel behavior based on our data:
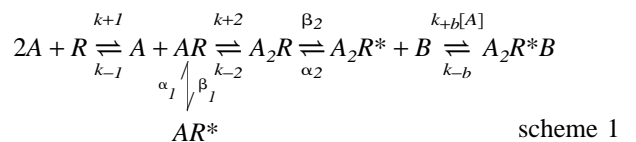
$$2A + R \underset{k-1}{\overset{k+1}{\rightleftharpoons}} A + AR \underset{k-2}{\overset{k+2}{\rightleftharpoons}} A_2R \underset{\alpha_2}{\overset{\beta_2}{\rightleftharpoons}} A_2R^* + B \underset{k-b}{\overset{k+b[A]}{\rightleftharpoons}} A_2R^*B$$

$$\alpha_1 \Big\Uparrow \beta_1$$

$$AR^* \qquad\qquad \text{scheme 1}$$

Table. Summary of Channel Properties

Receptor type	γ (pS)[a]	Reversal potential (mV)[a]	$\tau_{o,2}$(msec)[b]	$\gamma - Q^c_{10}$	$\tau_o - Q_o{}^c$
Wt	65 ± 4 (9;4)	−3	0.6 ± 0.2 (11)	1.5 ± 0.4 (6)	3.7 ± 0.6 (9)
α418Ala	68 ± 5 (8;2)	−1	0.4 ± 0.1 (8)	1.3 ± 0.2 (3)	3.4 ± 0.6 (2)
α418Gly	69 ± 5 (7;2)	−0.5	0.5 ± 0.1 (8)	1.1 ± 0.1 (7)	2.5 ± 0.4 (7)
α418Ser	61 ± 8 (2;1)	−5	0.8 ± 0.3 (3)	1.2 ± 0.2 (2)	2.4 ± 0.5 (2)
β447Trp	68 ± 4 (6;3)	−5	1.2 ± 0.6 (10)	1.3 ± 0.2 (3)	3.8 ± 0.5 (3)
α418Phe	69 ± 5 (7;3)	−3	1.7 ± 0.5 (12)	1.4 ± 0.4 (2)	3.3 ± 0.4 (2)
α418Trp	66 ± 2 (7;3)	3	15.8 ± 5.2 (6)	1.2 ± 0.4 (2)	3.5 ± 0.5 (2)
α418Trp + β447Trp	65 ± 2 55 ± 3 40 ± 4 (9;4)	0[d]	34.9 ± 5.9 (2)	1.7 ± 0.3 (2)[d]	2.5 ± 0.3 (2)[d]

All ± values are SD from the mean values except as otherwise indicated. (*a*) Mean conductance values and reversal potentials were calculated from regression lines (±SE) fitted to current-voltage curves containing all the points from individual patches pooled together for each receptor type. Recorded at potentials between −120 and −40 mV. The temperature was 13 ± 1°C with the exception of αAla-418 that was recorded at 16 ± 1°C. The numbers in parentheses are: number of oocytes; number of oocyte batches used. Sampled at 100 μsec. (*b*) Average of all the patches recorded at −80 mV and 13°C for each mutation with the exception of αAla-418 that was recorded at 16°C. Numbers in parentheses correspond to the number of patches. (*c*) Calculated from equation $Q_{10} = exp(10/\Delta T\ ln\ K_1/K_2)$, where K_1 and K_2 are mean values of γ or τ_o at each temperature. The number of patches are shown in parentheses. All the measurements were done at a holding potential of −80 mV and at temperatures between 12°C and 22°C. (*d*) Calculated from patches containing the high and intermediate conductance openings.

where R is the receptor, A is ACh, A_2R is the bi-liganded species, AR^* and A_2R^* are the monoligated and biliganded open state of the receptor-ligand complex, B is the blocker molecule (in this case ACh), and A_2R^*B is the blocked state of the complex, k_{+1} and k_{+2} are the binding rate constants and k_{-1} and k_{-2} are the first and second dissociation rate constant for the first and second binding sites (respectively), α_1 and α_2 are the fast and slow closing rate constants, β_1 and β_2 are the fast and slow opening rates, k_{+b} is the blocking rate, and k_{-b} is the rate of opening from the blocked state.

The resulting increase in the α418Trp open probability distribution can be seen in Fig. 6*A* for bursts recorded in the presence of 50 μM ACh. Occasional bursts with significantly higher or lower P_o than the mean open probability value could be seen for both channel types in most patches, presumably reflecting a different state or activation pathway of the channel. However, these accounted for a small percentage (~3%) of the openings, and were not included in the analysis. Figure 6*B* presents the burst mean open probability, P_o, as a function of ACh concentration. WT channels showed significantly smaller P_os from α418Trp channels at all the concentrations examined. Even at 100 μM, the highest concentration tested for WT, the P_o values were significantly lower than those measured for α418Trp even at 4 μM

ACh. Although increasing the ACh concentration had a bigger effect on the P_o of the mutant channels than on the WT, the relative EC_{50}s obtained from fits to Eq. 1 of both channel data sets remained similar to the values previously calculated from voltage-clamp data (Lee et al., 1994). Using a Hill coefficient of 1.8, the calculated EC_{50} values were 35 ± 5 μM (range of 21 to 50 μM) for WT channels and 10 ± 1 μM (range of 8 to 12 μM) for α418Trp. In contrast to our previous calculations from whole-cell recordings, the EC_{50} values from both channel types are significantly different from each other. These differences in EC_{50}s between mutant and WT channels are most likely a consequence of the changes in channel isomerization rates (α and β), although possible changes in the effective binding properties of the mutated channels cannot be ruled out.

At limiting low agonist concentrations, fast closures have been interpreted to represent channel activation rates. We did not use limiting low ACh concentrations in this study because the expression level was too low to record enough single channel events to compare both channel types. Fast closures at 1 and 4 μM ACh showed a mean duration of 0.03 msec for both mutant and WT channels (*see* Fig. 5). At these agonist concentrations the contamination by channel block in the WT channel is minimal (k_i for block has been calculated ~0.9 mM for
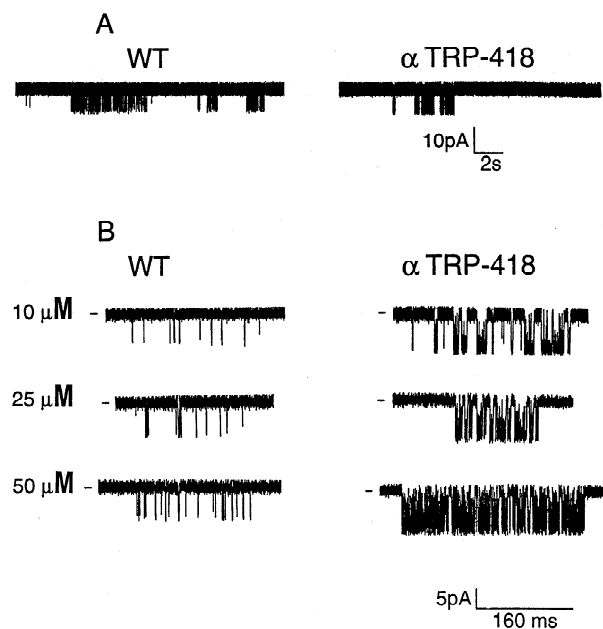
A

WT   α TRP-418

10pA |
       2s

B

WT   α TRP-418

10 μM -

25 μM -

50 μM -

5pA |_____
      160 ms

Fig. 4. Records of bursts from WT (left) and α418Trp (right) channels. (*A*) Compressed records from both receptor types showing bursts clustering over a ~20 second period. The ACh concentration was 50 μM in both cases. (*B*) Bursts at three different ACh concentrations for each receptor type show qualitatively the changes in the intraburst closed and open intervals as the agonist concentration is increased.

Torpedo channels expressed in fibroblasts by Sine et al. (1990); ~2.7 mM in BC3H-1 cells by Sine and Steinbach (1984); and ~1.3 mM in muscle by Ogden and Colquhoun (1985), so we believe this component is providing information about channel activation rates. Furthermore, this component does not change in weight or in value until ACh concentrations higher than 25 μM are reached. In mutant channels, on the other hand, fast closures due to channel block (as estimated from Fig. 9), can contribute significantly to this component even at 4 μM ACh, which makes any association of these values to activation processes untenable.

The major, slow component of the intraburst closed interval distributions that depended on ACh concentration (*see* Fig. 5) reflects channel activation characteristics, even though it bears no clear relationship to any of the microscopic rate constants in the activation scheme at the concentration range used for these experiments. The inverse of the mean closed time duration of this component will be called the effective opening rate, β'. Figure 7 shows β' values calculated at different ACh concentrations for both WT and α418Trp receptors. At all concentrations tested, β' values from α418Trp channels were significantly larger than for WT channels. At higher concentrations this difference became more marked going form a 3-fold change at 4 μM (2.5 sec^{-1} for WT and 8 sec^{-1} for α418Trp), to a 5-fold change at 50 μM (160 sec^{-1} for WT and 725 sec^{-1} for α418Trp). To

calculate the maximum opening rate, β, independently from the low agonist concentration measurements, saturating ACh concentrations at which β' reaches the agonist-independent isomerization rates would have been necessary (Auerbach, 1993). That level of saturation could not be achieved at the concentration range used for these experiments. Furthermore, the effect of channel block by ACh at high concentrations also interferes with the calculation of β. However, even though we were not able to calculate channel opening rates of either channel, there seem to be clear differences between their effective opening rates. These differences in β' are most likely a reflection of changes in the reaction rates along the activation pathway (i.e., agonist binding steps and/or opening rate) of the mutant channels.

EFFECTS ON PORE PROPERTIES

Channel Conductance

Figure 8 shows current amplitude histograms for WT, α418Trp, and α418Trp/β447Trp measured at −100 mV. All three distributions have peaks near 6 pA. None of the single amino acid substitutions in either the α or β subunit alone showed any significant change in single-channel conductance or the temperature dependence of conductance compared to WT channels, as shown in the Table. Q_{10} values for the conductance are consistent with the temperature coefficient for diffusion of ions in solution (Dilger et al., 1991; Hille, 1992). There was also no apparent change in selectivity since there were no appreciable changes in the reversal potentials given in the Table for any of the mutations.

In contrast to the single amino acid mutations, patches containing the α418Trp/β447Trp mutant showed up to three discernible conductance levels, as shown in Figs. 2, 8, and the Table. The subconductances were present normally with a low frequency in around 30% of all the patches expressing the α418Trp/β447Trp mutant channels and their appearance was not dependent on any particular voltage. The amplitude of the 40 pS subconductance level was too close to the amplitude of stretch-activated channels, endogenous in the oocyte membranes, to be differentiated at potentials less negative than −60 mV. To reduce the probability of having stretch-activated openings, the outside-out configuration was used (Methfessel et al., 1986). These outside-out patches showed events similar in appearance, amplitude and frequency of openings as the ones seen in the on-cell patches for the α418Trp/β447Trp.

Open Channel Block by ACh

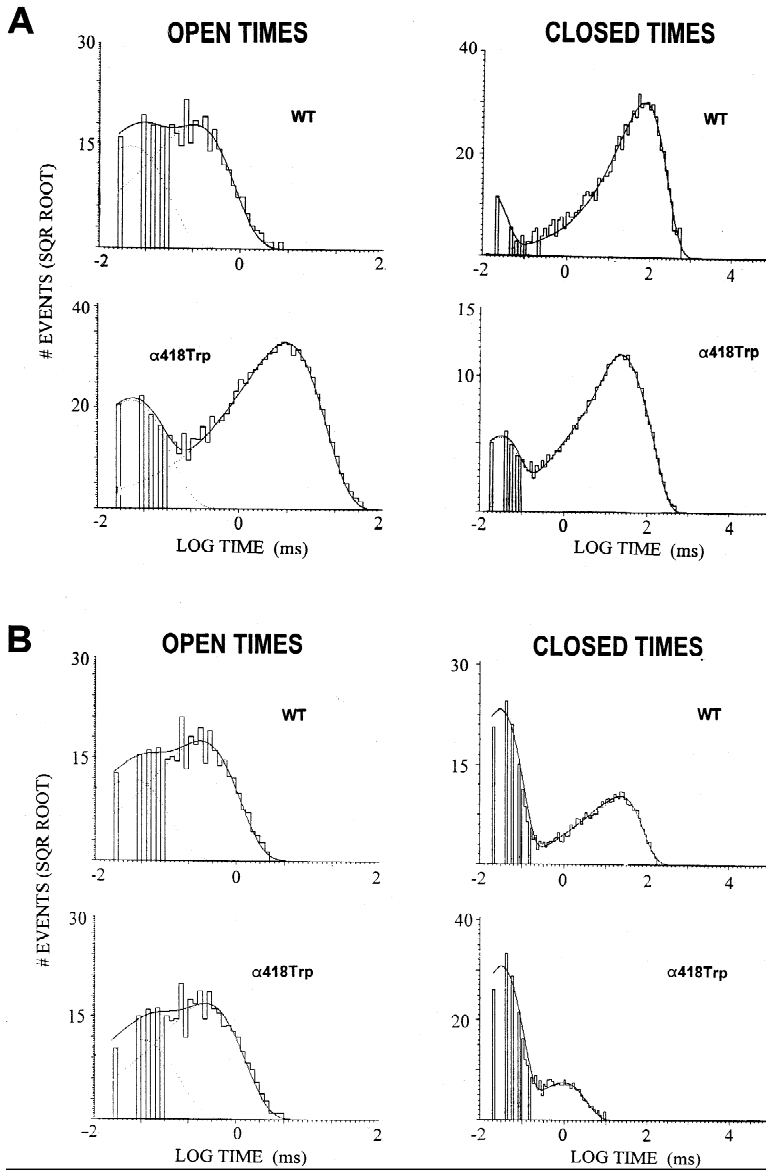Figure 9 shows the dependence on agonist concentration of the apparent closing rate constants, α_1 and α_2, for WT

A

B

Fig. 5. Open and closed time distributions for WT and α418Trp channels at (*A*) 4 μM and (*B*) 50 μM ACh. Distributions were constructed from single representative patches using IPROC3 and fitted by PSTAT6 software. Open-time distributions were fitted by the sum of two exponentials for both channel types. At 4 μM ACh, the fast components showed mean open times ($\tau_{o,1}$) of 0.06 ± 0.03 msec (fractional area, f = 0.45) and 0.03 ± 0.02 msec (f = 0.29) for WT and mutant channels respectively. The slower component ($\tau_{o,2}$) showed values of 0.21 ± 0.07 msec (f = 0.55) for WT and 4.54 ± 0.6 msec (f = 0.71) for α418Trp channels. At 50 μM ACh, $\tau_{o,1}$ were equal to 0.04 ± 0.03 msec (f = 0.35) and 0.03 ± 0.02 msec (f = 0.32) for WT and mutant channels respectively. $\tau_{o,2}$ were equal to 0.27 ± 0.04 msec (f = 0.65) for WT and 0.90 ± 0.1 msec (f = 0.68) for α418Trp channels. The closed time distributions were fitted by the sum of two to four exponentials. At 4 μM ACh, the fast component ($\tau_{c,1}$) showed a mean closed time equal to 0.033 ± 0.013 msec (f = 0.12) for WT and 0.045 ± 0.020 (f = 0.32) for α418Trp channels. At 50 μM ACh, $\tau_{c,1}$) was equal to 0.030 ± 0.02 msec (f = 0.20) and 0.032 ± 0.02 msec (f = 0.89) for WT and mutant channels respectively. The slower envelope of closings was fitted by two to three exponentials. The WT closed time distribution at 4 μM was best fitted by the sum of two exponentials: 2.50 ± 0.9 msec (f = 0.02) and 96.30 ± 3.1 msec (f = 0.75). At the same ACh concentration, the mutant channels closings were best fitted by the sum of three components: 0.56 ± 0.05 ms (f = 0.015), 67.79 ± 1.60 msec (f = 0.64), and 376.66 ± 8.10 msec (f = 0.02). At 50 μM ACh, WT channels closed time distributions showed two components with mean values equal to 2.88 ± 0.7 msec (f = 0.02) and 22.58 ± 0.8 msec (0.78). At the same ACh concentration, the mutant channels also showed two components with mean values of 0.93 ± 0.21 msec (f = 0.10) and 4.96 ± 0.3 msec (f = 0.01). The data was filtered at 10 kHz and sampled at 20 μs per point.

and α418Trp channels calculated from the inverse of corrected mean open times. There is essentially no change in α_1 between both channel types. Linear regressions fitted individually to both data groups up to 50 μM showed slopes not significantly different from zero. Mean values for α_1 were obtained from the intercept in the ordinate axis of each regression line. Those were 47,000 ± 8200 sec^{-1} for WT and 50,000 ± 9700 sec^{-1} for α418Trp. Changes in the apparent slow closing rate, α_2 with agonist concentration were not significant for WT channels up to 100 μM ACh. However, a slight constant increment (though uncertain) was detected at moderately high concentrations for these channels. An apparent slow closing rate (α_2) of 4152 ± 53 sec^{-1} was obtained from the fit of a regression line to the WT data from

concentrations below 25 μM. When data acquired at concentrations higher than 25 μM were fitted by a regression line, a small increase in the slope (blocking rate) of 12 ± 2 μMsec^{-1} was obtained. The mutant channel, on the other hand, exhibits a significant increase in the apparent closing rate, α_2, that is not associated with any decrease in its conductance (*see* Fig. 4). Assuming that the increase in the measured closing rate, α_2, was caused by a component due to ACh blocking events, the rate of block, $k_{+b}[\text{ACh}]$, and the value of the closing rate, $\alpha_{2,\text{real}}$, independent of block can be calculated from the α418Trp data, using the relation

$$\alpha_2 = \alpha_{2,\text{real}} + k_{+b}[\text{ACh}] \qquad (2)$$

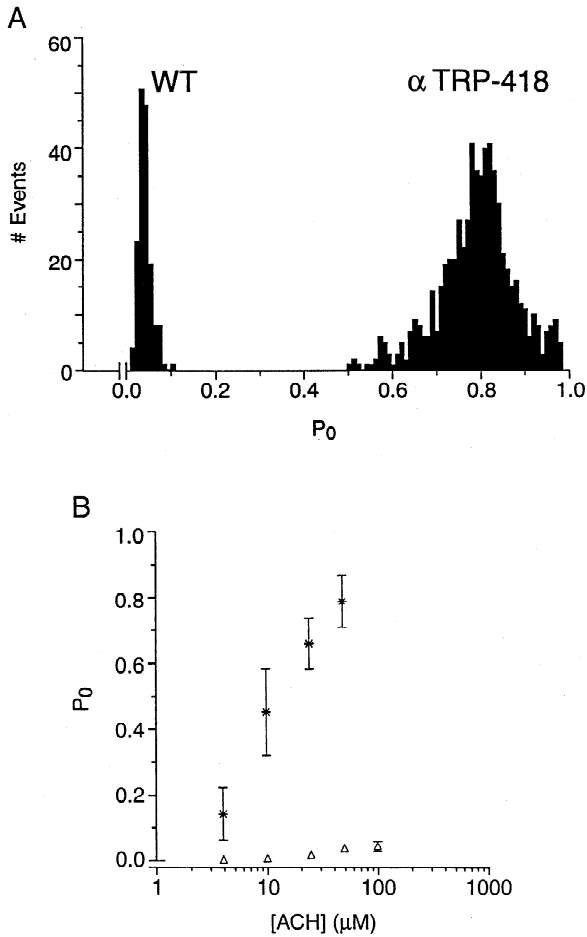An estimation of the blocking rate, $k_{+b}[\text{ACh}]$, was ob-

A

B

Fig. 6. Burst open probability is significantly different for WT and α418Trp receptors. (*A*) Open probability distribution for WT and α418Trp at 50 μM ACh, −100 mV and 18°C. The number of events in the ordinate refers to the number of bursts. Each histogram was constructed from a single patch. (*B*) Open probability dependence on ACh concentration for WT (Δ) and α418Trp (*) channels. Every point comes from the mean P_o value ± SE of one to three representative patches like the ones shown in section *A*. The errors are within the range of the symbol size used for those points not showing error bars.

Fig. 7. Effective opening rate (β′) dependence on ACh concentration for WT (▲) and α418Trp (*) channels. β′ was calculated as the inverse of the major slow component in the closed time distributions (*see* the text for further details about β′ estimation). Data comes from the same patches used in the P_o calculations presented in Fig. 6.

tained initially by fitting the α418Trp data. This value was calculated to be 58.7 ± 0.1 $\mu M^{-1}sec^{-1}$. The best fit to the data (*see* the dotted curve in Fig. 9) was obtained with a slope of 55 $\mu M^{-1}sec^{-1}$ and an intercept in the ordinate axis of 120 sec^{-1}. The $\alpha_{2,real}$ derived from this fit is not significantly different from the value obtained for α_2 at ACh concentrations of 1 μM (198 ± 10 sec^{-1}).

The short duration closed times component that is assumed to represent activation of channels in the A_2R state at limiting low concentrations showed a substantial increase in its weight at higher ACh concentrations in the mutant channels. This increase, which is sensitive to membrane hyperpolarization (*not shown*), can be accounted for most readily if it is assumed to represent
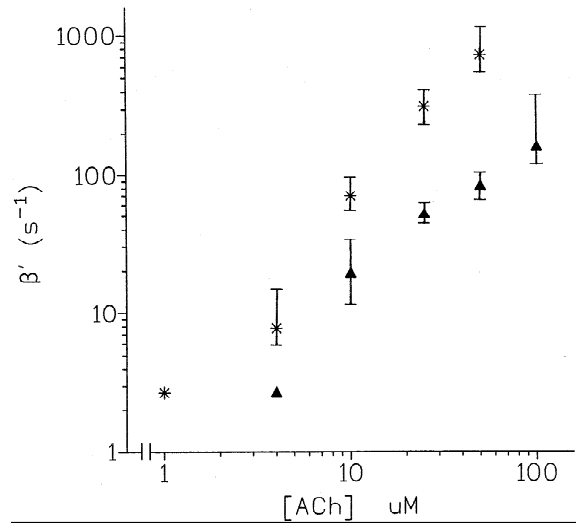
channel blocking events (Sine & Steinbach, 1984). If we assume that a channel in the A_2R^* state can only go to the blocked state or to the close state A_2R, then, at high agonist concentrations, where the blocking rate >>> closing rate (α_2), this component should be composed preferentially of blocking events. For WT channels, concentrations in excess of 350 μM must be reached in order for the blocking rate to exceed the channel closing rate. In the α418Trp mutant, only 3 μM ACh is sufficient to make both rate constants equal, a more than 100-fold difference. At 50 μM ACh, mutant channels in the A_2R^* state will tend to go ~24 times more often to the blocked state than to the closed state. Based on the above discussion, this rate should mostly reflect the unblocking rate of the channel (k_{-b}). The inverse of the fast closed time constant was calculated to be $71,429 \pm 15,000$ sec^{-1}. This value is similar to the unblocking rate for *Torpedo* channels expressed in fibroblasts, calculated to be ~80,000 sec^{-1} by Sine et al. (1990). From the ratio of k_{+b}/k_{-b}, the dissociation constant for the blocking site in the mutant channels should be then ~1.3 mM, which is close to the 0.9 mM value reported by Sine and collaborators (1990). The calculation of k_{-b}, again, is limited by our system resolution as it is reflected by the higher error obtained on its calculation. WT channels were less sensitive to channel block at all the concentrations tested. The difference in sensitivity to channel block between WT and mutant channels could be a consequence of their differences in open durations, although changes in the structure of the pore or vestibule producing a greater accessibility for the ligand to the blocking site of the receptor are also possible.
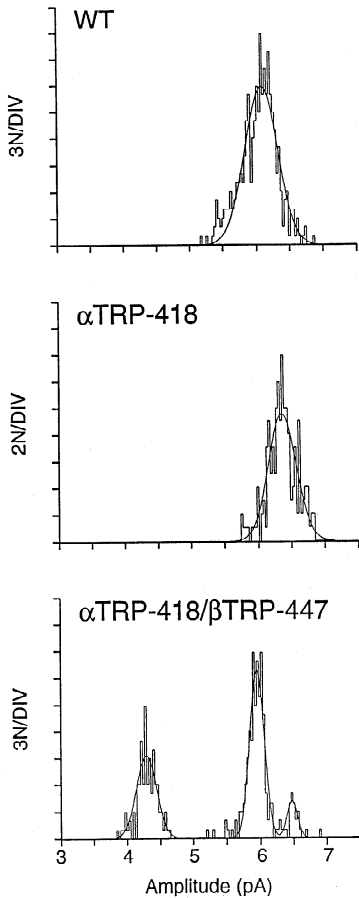
Fig. 8. Amplitude distribution histograms from single patches containing WT, α418Trp and from two patches expressing the α418Trp/β447Trp receptors. The current values used to fit the histograms were: 6.2 pA for WT (300 events), 6.4 pA for α418Trp (167 events), and 4.3, 5.9 and 6.5 pA as the small, intermediate and high conductance values for α418Trp/β447Trp mutant (316 events). The predominant component in α418Trp/β447Trp amplitude distributions varied from patch to patch between the high and intermediate amplitude. In most patches, though, only one or two of the three amplitude levels were present at the same time. The files used in generating these distributions were from on-cell patches maintained at 13°C, filtered at 4 kHZ and sampled at 100 μsec. The ACh concentration was 1 μM for the triple-mutant, and 4 μM for the other two distributions; the holding potential was −100 mV in all the cases.

Discussion

The highly hydrophobic M4 transmembrane domain of the nAChR is the least evolutionary conserved of the four domains composing the acetylcholine receptor (Devillers-Thiery et al., 1983; Noda et al., 1983). Its preferential labeling by nonspecific lipophilic probes made it the most likely candidate to be placed at the protein-lipid interface in receptor topology models (Blanton & Cohen, 1992). We have previously shown that single amino acid substitutions in this domain can
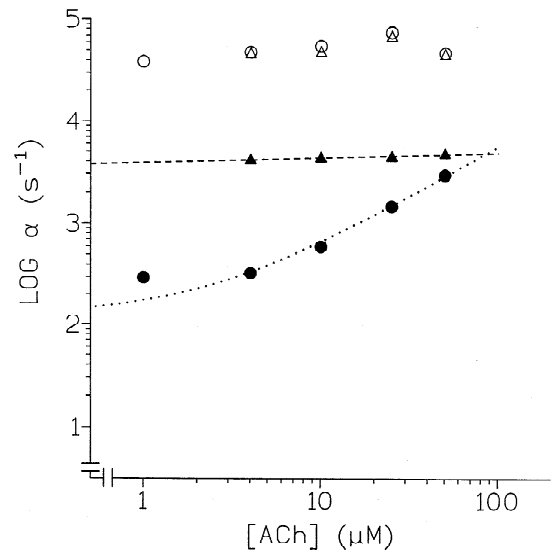

Fig. 9. Agonist dependence of fast ($α_1$, open symbols) and slow ($α_2$, filled symbols) closing rates. Shown are measured closing rate values obtained from the inverse of mean open times inside a burst for concentrations ≥10 μM and total mean open times at concentrations ≤4 μM. Contrary to WT (▲) channels, the slow closing rate for α418Trp (●) increased significantly with ACh concentrations higher than 4 μM. The dashed line on the WT is a linear regression fit to the data in between 10 and 50 μM. This line has a slope of $12.2 ± 1.8$ μM^{-1}s^{-1} and intercepts the ordinate axis at 4,152 sec^{-1} ± 52.7 sec^{-1} (two tailed, $P =$ .02). For the α418Trp data, the points between 10 and 50 μM were fitted also by a linear regression which gave a slope of $58.7 ± 0.1$ μM^{-1}s^{-1} and an ordinate intercept of $10 ± 3.5$ sec^{-1}. The dotted curve was constructed from equation (2) using the values $α_{2,real} = 120$ sec^{-1} and $k_{+b}[A] = 55$ μM^{-1}s^{-1}. No significant differences were seen between WT (△) and α418Trp (○) fast closing rates. Linear regression fits to both data sets showed slopes not significantly different from 0. The intercept in the ordinate axis was $47,054 ± 8190$ sec^{-1} for WT channels and $49,951 ± 9,690$ sec^{-1} for the mutant channels. Every point corresponds to a single patch exposed to identical recording conditions. In this case the temperature was $18 ± 1$°C. The number of bursts used in these calculations were for WT: at 4, 10, 25, 50 and 100 μM; 6, 273, 77, 163, and 31 respectively. For α418Trp: at 4, 10, 25, and 50 μM; the number of bursts were 207, 131, 34 and 526 respectively.

alter the activity of ACh induced macroscopic currents in *Xenopus* oocytes (Lee et al., 1994). In the current work, we present a more detailed single-channel data analysis of the mutations in the α418Cys position and extend our analysis to include the M4 domain in the β-subunit. Of the five different amino acids we tested as replacements for the wild type α418Cys, only phenylalanine and tryptophan substitutions significantly affected channel open times. Replacing the α418Cys with tryptophan resulted in a substantial increase in the channel open probability, due to increases (up to thirtyfold) in their mean open times and up to a tenfold increase in their effective opening rates. The α418Phe mutation or replacement of the homologous β447Cys with tryptophan increased channel open times two to threefold. The changes seen in chan-

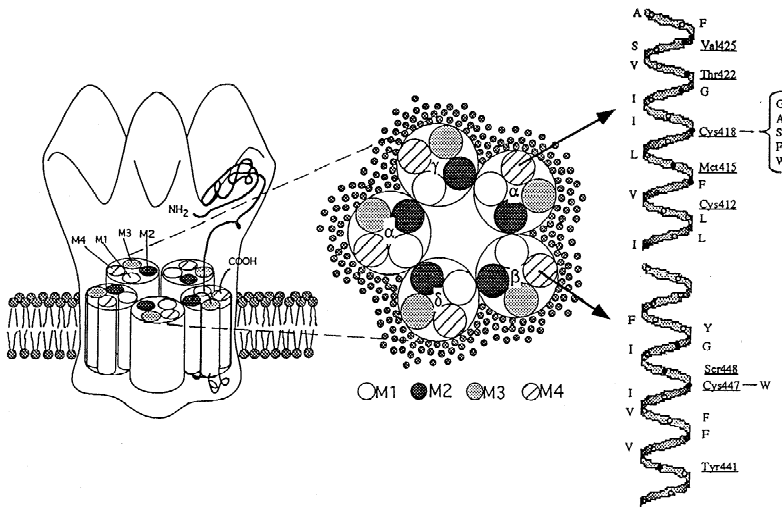**Fig. 10.** Topological representation of α418Cys and β447Cys positions within the nicotinic acetylcholine receptor and in relation to their surrounding lipid bilayer. Underlined residues are labeled by ^{125}I-TID.

nel gating properties for the α418Trp receptor are sufficient to account for the threefold increase in maximal ACh response seen for this mutation in our previous whole-oocyte measurements (Lee et al., 1994). The fact that we did not see larger changes in the ACh-induced macroscopic currents carried by mutant channels is probably due to a higher incidence of open channel block and/or an increase in their rate of desensitization.

In our previous paper we had proposed that the changes in the closing rate constant of the mutated channels were of enough magnitude to totally account for the changes seen at the macroscopic level. The present experiments with high ACh concentrations and the study of burst kinetics for WT and α418Trp channels allowed us to expand our previous model. Scheme 1 incorporates the presence of two possible activation pathways and channel block into the kinetic model.
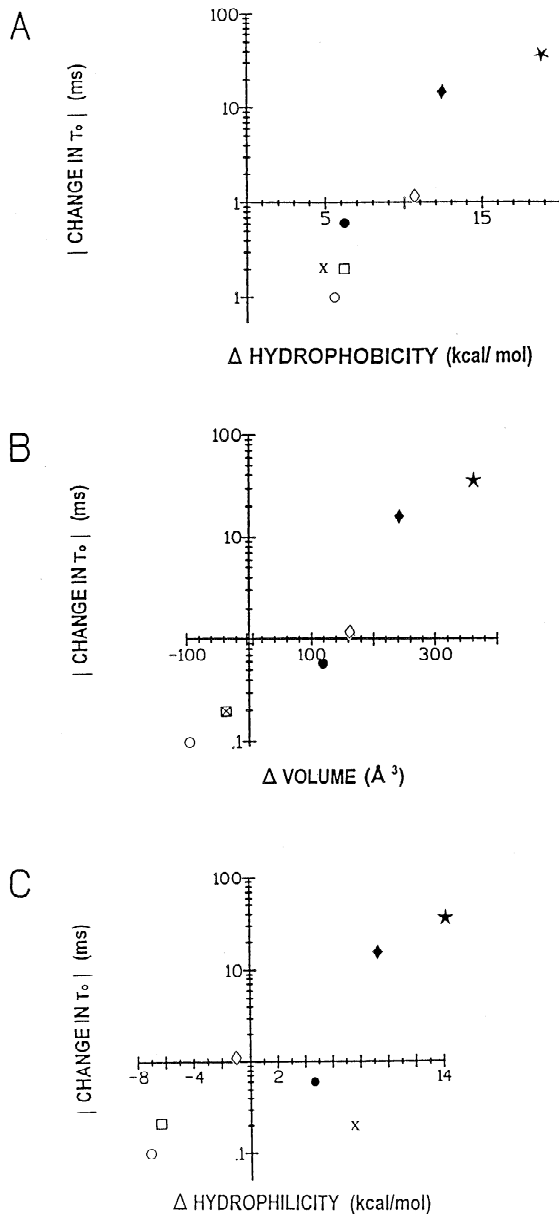
The preference of the mutated channels to stay in the open conformation compared to WT channels makes the block by ACh more visible in them. This open channel block, together with the occurrence of subconductance states in the α418Trp/β447Trp mutant are two detected changes in the properties of the pore. Also, even though we did not look at the binding properties in this study, there are two factors suggesting that some changes in these binding properties might have happened. First, we found significant differences in the EC_{50}s calculated from the open time probabilities between the mutant and WT channels, in contrast to our previous EC_{50} calculations from macroscopic currents. Second, even though the β/α ratio is changing in the mutant channels respect to WT channels (~40 times), that difference did not parallel the change in EC_{50}s of ~3.5 times between both channels types. Thus, since EC_{50}s are dependent on channel gating as well as on channel binding (Colquhoun & Ogden, 1988), some changes in the binding properties could account for this divergence. Considering that the

place we are mutating is not in close proximity to the M2 membrane spanning region, lining the channel pore (Hucho et al., 1986; Imoto et al., 1986, 1988), or close to the ligand binding site, we have to postulate that the gating properties being modified by our amino acid substitutions must be controlled by allosteric interactions between different structural components of the channel protein. This sort of long range interaction in channel gating had been postulated long ago between the binding site and the ion pore (Monod, Changeux & Jacob, 1963; Hertz, Johnson & Taylor, 1989; *see* review by Lena & Changeux, 1993).

Rather than a generalized disruption of channel structure, the alterations we observe in channel gating are likely due to localized or specific effects on channel conformation since other permeability properties did not change in the mutant channels. None of the mutations studied showed any apparent change in selectivity or in the magnitude of the main conductance state. Also, mutations of nearby residues in M4 (α412Cys and α421Gly) to tryptophan had a minor or no effect on channel open times (Lasalde et al., 1996).

Other amino acid substitutions at conserved and lipid exposed positions in M4 are in progress that will allow us to describe the mechanism of action by which these substitutions modify channel kinetics. However, we can postulate some possibilities that are consistent with our current data.

Hydrophobic interactions between the side chain and membrane lipids might be expected to be important for the function of the α418Cys residue, which is exposed to the lipid environment based on labeling studies (Blanton & Cohen, 1992, 1994) (*see* Fig. 10). Figure 11A shows a positive correlation between the changes in relative hydrophobicity and the changes in ($\tau_{o,2}$) expressed by all the different amino acid substitution made. However, hydrophobicity does not seem to be the only

A

B

C

Fig. 11. Correlation between some amino acid properties (relative to cysteine), and the absolute change in mean open time for all the substitutions at position α418Cys and β447Cys. Every mutation is represented by a different symbol as follows: (♦) α418Trp; (◇) α418Phe; (X) α418Ser; (○) α418Gly; (□) α418Ala; (●) β447Trp; and (☆) α418Trp/β447Trp. The changes in mean open time were calculated from the values shown in the Table. (A) Correlation between the change in side chain relative hydrophobicity and the absolute change in mean open time. The hydrophobicities of the side chains were measured by their distribution between a nonpolar environment: either ethanol or dioxane and water. The value for cysteine was calculated from its surface area and corrected for the fraction of nonionized form present at pH7. (B) Correlation between the change in side chain volume and the absolute change in mean open time. (C) Correlation between the change in side chain relative hydrophilicity and the absolute change in mean open time. Hydrophilicities were defined as RT in (K_{eq}/α), where K_{eq} is the distribution coefficient between H_2O and vapor for a small molecule representing the side chain of the amino acid, and α is the fraction the nonionized form of the amino acid at pH7. All hydrophilicities were expressed relative to that of glycine. Hydrophilicity and relative hydrophobicity values for the side chain groups were obtained from Creighton (1983). The side chain volumes were obtained from Chothia (1975).

(Ser) or a less polar residue (Ala) had no effect on open times (*not shown*).

A strong positive correlation between changes in $\tau_{o,2}$ and changes in size or volume of the substituted residues at position α418 and β447 can be seen in Fig. 11*B*. The changes in the side chain volume, relative to cysteine, correlated qualitatively with the relative changes in mean open times for the different residues tested (*see* Table). This relation which is more apparent for changes to the bigger aromatic residues, extends to include the number of subunits modified during the process of amino acid substitutions. The increase in channel open time that the tryptophan replacements caused in one (β), two (α) or three (2 α + β) subunits suggest that both α and β subunits participate during channel closing. Furthermore, assuming that the effect on open time is equally caused by both mutated α subunits, the changes in free energy that all the Trp mutations showed respect to WT channels suggest that each subunit contributes independently and additively to the process of channel closing. Recently, two other studies have demonstrated that each of the Leu 9′ residues on the M2 domain participate independently and symmetrically in a key step during the structural transition(s) between the closed and open state of the channel (Labarca et al., 1995; Filatov & White, 1995). In an analogous study, Lo, Pinkham & Stevens, (1991) found a similar pattern of dependence on the size of the substituted residue for an M1 site normally occupied by a cysteine on murine AChRs. These authors also found a significant contribution of the γ subunit to the control of channel closure.

The importance of channel regulation through lipid-protein interactions has been recognized for a long time.

determinant of the changes in channel gating. Although changes to more hydrophobic residues like tryptophan and phenylalanine induced the biggest effects in open times, changes to more hydrophilic residues like alanine or glycine did not affect them (*see* Fig. 11*C*). No clear correlation was seen between the relative changes in hydrophilicity and channel open times. Also the effect in $\tau_{o,2}$ is not exclusively or linearly correlated to the hydrophobic properties of the substituted amino acid since Phe hydrophobicity is closer to the Trp hydrophobicity that what we would expect from its effect in open time. Finally, the polarity of the residue at α418 does not seem to be critical in determining channel gating properties since mutations of the cysteine to a more polar residue

Noncompetitive blockers have been shown to bind to several low affinity sites per molecule of nAChR, enhancing the affinity of the receptor for its ligands and accelerating their desensitization (Cohen, Weber & Changeux, 1974; Oswald, Heidmann & Changeux, 1983). These low affinity sites are thought to lie at the receptor-membrane interface since the ligands are generally lipophilic and the number of sites are dependent on the lipid-to-protein ratio in reconstitution experiments (Heidmann, Oswald & Changeux, 1983). Other molecules like general anesthetics, some local anesthetics, phospholipases, detergents and fatty acids are able to enhance both the rate of desensitization and the affinity of the receptor for its ligands (*reviewed* in Ochoa et al., 1989; Lena & Changeux, 1993). Lipids and lipid-perturbing agents have been also shown to block the ACh induced activity in reconstituted microsacs (Criado, Eibl, & Barrantes, 1982; Anholt et al., 1982; McNamee & Ochoa, 1982; Earnest & McNamee, 1984; Fong & McNamee, 1986) and modify the channel activity in myocytes (Lasalde et al., 1995). The results of our substitution experiments in the transmembrane M4 domain of the nicotinic acetylcholine receptor further support the notion that the lipid environment may well be regulating the properties of these receptors through indirect modifications of conformational transitions between its different states.

References

Anand, R., Conroy, W.G., Schoepfer, R., Whiting, P., Lindstrom, J. 1991. Neuronal nicotinic acetylcholine receptors expressed in *Xenopus* oocytes have a pentameric quarternary structure. *J. Biol. Chem.* **266:**11192–11198

Anholt R., Fredkin, D.R., Deerink, T., Ellisman, M., Montal, M., Lindstrom, J. 1982. Incorporation of acetylcholine receptors into liposomes. Vesicle structure and acetylcholine receptor function. *J. Biol. Chem.* **257:**7122–7134

Auerbach, A. 1993. A Statistical analysis of acetylcholine receptor activation in *Xenopus* myocytes: Stepwise versus concerted models of gating. *J. Physiol.* **461:**339–378

Auerbach, A., Lingle, C.J. 1986. Heterogeneous kinetic properties of acetylcholine receptor channels in *Xenopus* myocytes. *J. Physiol.* **378:**119–140

Blanton M.P., Cohen, J.B. 1992. Mapping the lipid-exposed regions in the *Torpedo californica* nicotinic acetylcholine receptor. *Biochemistry.* **31:**3738–3750

Blanton M.P., Cohen, J.B. 1994. Identifying the lipid-protein interface of the *Torpedo* nicotinic acetylcholine receptor: secondary structure implications. *Biochemistry.* **33:**2859–2872

Changeux, J.-P., Devillers-Thiery, A., Galzi, J.L., Bertrand, D. 1992. New mutants to explore nicotinic receptor functions. *Trends Pharmacol. Sci.* **13:**299–301

Chothia, C. 1975. Structural invariants in protein folding. *Nature* **254:**304–308

Clarke, J.H., Martinez-Carrion, M. 1986. Labeling of functional sensitive sulfhydryl-containing domains of acetylcholine receptor from *Torpedo californica* membranes. *J. Biol. Chem.* **261:**10063–10072

Cohen, J.B., Weber, M., Changeux, J.-P. 1974. Effects of local anesthetics and calcium on the interaction of cholinergic ligands with the nicotinic receptor protein from *Torpedo marmorata. Mol. Pharmacol.* **10:**904–932

Colquhoun, D., Hawkes, A.G. 1981. On the stochastic properties of single ion channels. *Proc. R. Soc. Lond. B.* **211:**205–235

Colquhoun, D., Ogden, D.C. 1988. Activation of ion channels in the frog endplate by high concentrations of acetylcholine. *J. Physiol.* **395:**131–159

Colquhoun, D., Sakmann, B. 1981. Fluctuations in the microsecond time range of the current through single acetylcholine receptor ion channels. *Nature* **294:**464–466

Colquhoun, D., Sigworth, F.J. 1983. Fitting and statistical analysis of single-channel records. In: *Single-Channel Recording.* Second edition. B. Sakmann, and E. Neher, editors. pp. 254–257. Plenum Press, New York

Cooper, E., Couturier, S., Ballivet, M. 1991. Pentameric structure and subunit stoichiometry of a neuronal nicotinic acetylcholine receptor. *Nature.* **350:**235–238

Creighton, T.E. 1983. Physical forces that determine the properties of properties. In: *Proteins; Structure and Molecular Properties.* pp. 133–157. W.H. Freeman, New York

Criado, M., Eibl, H., Barrantes, F.J. 1982. Effects of lipids on acetylcholine receptor. Essential need of cholesterol for maintenance of agonist-induced state transitions in lipid vesicles. *Biochemistry.* **21:**5750–5755

Devillers-Thiery, A., Giraudat, J., Bentaboulet, M., Changeux, J.-P. 1983. Complete mRNA coding sequence of the acetylcholine binding α-subunit of *Torpedo marmorata* acetylcholine receptor: a model for transmembrane organization of the polypeptide chain. *Proc. Natl. Acad. Sci. USA.* **80:**2067–2071

Dilger, J.P., Brett, R.S., Poppers, D.M., Liu, Y. 1991. The temperature dependence of some kinetic and conductance properties of acetylcholine receptor channels. *Biochim. et Biophys. Acta* **1063:**253–258

Earnest, J.P., Limbacher, Jr., H.P., McNamee, M.G., Wang, H.H. 1986. Binding of local anesthetics to reconstituted acetylcholine receptors: effect of protein surface potential. *Biochemistry.* **25:**5809–5818

Earnest, J.P., Wang, H.H., McNamee, M.G. 1984. Multiple binding sites for local anesthetics on reconstituted acetylcholine receptor membranes. *Biochem. Biophys. Res. Commun.* **123:**862–868

Filatov, G.N., White, M.M. 1995. The role of conserved leucines in the M2 domain of the acetylcholine receptor in channel gating. *Molec. Pharmacol.* **48:**379–384

Fong, T.M., McNamee, M.G. 1986. Correlation between acetylcholine receptor function and structural properties of membranes. *Biochemistry.* **25:**830–840

Fong, T.M., McNamee, M.G. 1987. Stabilization of acetylcholine receptor secondary structure by cholesterol and negatively charged phospholipids in membranes. *Biochemistry.* **26:**3871–3880

Galzi, J.-L., Revah, F., Bessis, A., Changeux, J.-P. 1991. Functional architecture of the nicotinic acetylcholine receptor: from electric organ to brain. *Annu. Rev. Pharmacol.* **31:**37–72

Giraudat, J., Galzi, J.L., Revah, F., Changeux, J.-P., Haymont, P., Lederer, F. 1989. The noncompetitive blocker [(3)H]chlorpromazine labels segment M2 but not segment M1 of the nicotinic acetylcholine receptor alpha-subunit. *FEBS Lett.* **253:**190–198

Giraudat, J., Montecucco, C., Bisson, R., Changeux, J.-P. 1985. Transmembrane topology of acetylcholine receptor subunits probed with photoreactive phospholipids. *Biochemistry.* **24:**3121–3127

Hamill, O.P., Marty, A., Neher, E., Sakmann, B., Sigworth, F.J. 1981. Improved patch-clamp techniques for high-resolution current recording from cells and cell-free membrane patches. *Pfluegers Arch.* **391:**85–100

Heidmann, T., Oswald, R.E., Changeux, J.-P. 1983. Multiple sites of action for noncompetitive blockers on acetylcholine receptor rich membrane fragments from *Torpedo marmorata. Biochemistry.* **22:**3112–3127

Hertz, J.M., Johnson, D.A., Taylor, P. 1989. Distance between the agonist and noncompetitive inhibitor sites on the nicotinic acetylcholine receptor. *J. Biol. Chem.* **264:**12439–12448

Hille, B. 1992. Elementary properties of ions in solution. In *Ionic Channels of Excitable Membranes.* Second edition. pp. 259–290. Sinauer Associates, Sunderland, MA

Horton, R.M., Pease, L.R. 1991. Recombination and mutagenesis of DNA sequence using PCR. In: *Directed Mutagenesis.* M.J. McPherson, editor. pp. 217–246. IRL Press, New York

Hucho, F., Oberthur, W., Lottspeich, F. 1986. The ion channel of the nicotinic acetylcholine receptor is formed by the homologous helices MII of the receptor subunits. *FEBS Lett.* **205:**137–142

Huganir, R.L., Racker, E. 1982. Properties of proteoliposomes reconstituted with acetylcholine receptor from *Torpedo californica. J. Biol. Chem.* **257:**9372–9378

Imoto, K., Busch, C., Sakmann, B., Mishina, M., Konno, T., Nakai, J.M., Bujo, H., Mori, Y., Fukuda, M., Numa, S. 1988. Rings of negatively charged amino acids determine the acetylcholine receptor channel conductance. *Nature* **335:**645–648

Imoto, K., Methfessel, C., Sakmann, B., Mishina, M., Mori, Y., Konno, T., Fukuda, K., Kurasaki, M., Bujo, H., Fujita, Y., Numa, S. 1986. Location of a δ-subunit region determining ion transport through the acetylcholine receptor channel. *Nature* **324:**670–674

Kao, P.N., Dwork, A.J., Kaldany, R.J., Silver, M.L., Wideman, J., Stein, S., Karlin, A. 1984. Identification of a subunit half-cystine specifically labeled by an affinity reagent for the acetylcholine receptor binding site. *J. Biol. Chem.* **259:**11662–11665

Karlin, A., Akabas, M.H. 1995. Toward a structural basis for the function of the nicotinic acetylcholine receptors and their cousins. *Neuron.* **15:**1231–1244

Labarca, C., Nowak, M.W., Zhang, H., Tang, L., Deshpande, P., Lester, H.A. 1995. Channel gating governed symmetrically by conserved leucine residues in the M2 domain of nicotinic receptors. *Nature.* **376:**514–516

Lasalde, J.A., Colom, A., Resto, E., Zuazaga, C. 1995. Heterogeneous distributions of acetylcholine receptors in chick myocytes induced by cholesterol enrichment. *Biochim. Biophys. Acta* **1235:**361–368

Lasalde, J.A., Tamamizu, S., Butler, D.H., Vibat, C.R.T., McNamee, M.G. 1996. Tryptophan substitutions at the lipid exposed transmembrane segment M4 of the *Torpedo* AChR governs channel gating. In press, *Biochemistry*

Lee Y-H., Li, L., Lasalde, J., Rojas, L., McNamee, M.G., Ortiz-Miranda, S.I., Pappone, P. 1994. Mutations in the M4 domain of *Torpedo californica* acetylcholine receptor dramatically alter ion channel function. *Biophys. J.* **66:**646–653

Lena, C., Changeux, J.-P. 1993. Allosteric modulations of the nicotinic acetylcholine receptor. *Trends in Neurosc.* **5:**181–186

Li, L., Lee, Y.-H., Pappone, P., Palma, A., McNamee, M.G. 1992. Site-specific mutations of the nicotinic acetylcholine receptor at the lipid-protein interface dramatically alter ion channel gating. *Biophys. J.* **62:**61–63

Li, L., Schuchard, M., Palma, A., Pradier, L., McNamee, M.G. 1990. Functional Role of the cysteine 451 thiol group in the M4 helix of the γ-subunit of *Torpedo californica* acetylcholine receptor. *Biochemistry.* **29:**5428–5436

Lo, D.C., Pinkham, J.L., Stevens, C.F. 1991. Role of a key cysteine residue in the gating of the acetylcholine receptor. *Neuron* **6:**31–40

McNamee, M.G., Ochoa, E.L.M. 1982. Reconstitution of acetylcholine receptor function in model membranes. *Neurosc.* **7:**2305–2319

Methfessel, C., Witzemann, V., Takahashi, T., Mishina, M., Numa, S., Sakmann, B. 1986. Patch clamp measurements on *Xenopus laevis* oocytes: currents through endogenous channels and implanted acetylcholine receptors and sodium channels. *Pfluegers Arch.* **407:**577–588

Monod, J., Changeux, J.-P., Jacob, F. 1963. Allosteric proteins and cellular control systems. *J. Mol. Biol.* **6:**306–329

Neil, J., Xiang, Z., Auerbach, A. 1991. List-oriented analysis of single channel data. *Methods in Neuroscience* **4:**474–490

Noda, M., Takahashi, H., Tanabe, T., Toyosata, M., Kikyotani, S., Furutani, Y., Hirose, T., Takashima, H., Inayama, S., Miyata, T., Numa, S. 1983. Structural homology of *Torpedo californica* acetylcholine receptor subunits. *Nature* **302:**528–532

Ochoa, E.L.M., Chattopadhyay, A., McNamee, M.G. 1989. Desensitization of the nicotinic acetylcholine receptor: Molecular mechanisms and effect of modulators. *Cellular and Molec. Neurobiol.* **9:**141–178

Ogden, D.C., Colquhoun, D. 1985. Ion channel block by acetylcholine, carbachol and suberyldicholine at the frog neuromuscular junction. *Proc. R. Soc. London B.* **225:**329–355

Oswald, R.E., Heidmann, T., Changeux, J.-P. 1983. Multiple affinity states for noncompetitive blockers revealed by [³H]phencyclidine binding to acetylcholine receptor rich membrane fragments from *Torpedo marmorata. Biochemistry* **22:**3128–3136

Pradier, L., McNamee, M.G. 1992. The nicotinic acetylcholine receptor. In: *The Structure of Biological Membranes.* P. Yeagle, editor. pp. 1047–1106. Telford, Caldwell, New Jersey

Pradier, L., Yee, A.S., McNamee, M.G. 1989. Use of chemical modifications and site-directed mutagenesis to probe the functional role of thiol groups on the gamma subunit of *Torpedo californica* acetylcholine receptor. *Biochemistry* **28:**6562–6571

Sachs, F., Auerbach, A. 1983. Single channel electrophysiology: use of the patch clamp. *Methods in Enzymology* **103:**147–176

Sachs, F., Neil, J., Barkakati, N. 1982. The automated analysis of data from single ionic channels. *Pfluegers Arch.* **395:**331–340

Sakmann, B., Patlak, J., Neher, E. 1980. Single acetylcholine-activated channels show burst-kinetics in presence of desensitizing concentrations of agonist. *Nature* **286:**71–73

Sine, S.M., Claudio, T., Sigworth, F.J. 1990. Activation of *Torpedo* acetylcholine receptors expressed in mouse fibroblasts. Single channel current kinetics reveal distinct agonist binding affinities. *J. Gen. Physiol.* **96:**395–437

Sine, S.M., Steinbach, J.H. 1984. Agonists block currents through acetylcholine receptor channels. *Biophys. J.* **46:**277–284

Sunshine, C., McNamee, M.G. 1992. Lipid modulation of acetylcholine receptor function: the role of neutral and negatively charged lipids. *Biochim. et Biophys. Acta* **1108:**240–246

Sunshine, C., McNamee, M.G. 1994. Lipid modulation of nicotinic acetylcholine receptor function: The role of membrane lipid composition and fluidity. *Biochim. Biophys. Acta* **1191:**59–64

Unwin, N. 1993. Nicotinic acetylcholine receptor at 9 Å resolution. *J. Molecular Biol.* **229:**1101–1124

Walker, J.W., Richardson, C.A., McNamee, M.G. 1984. Effects of thiol-group modifications of *Torpedo californica* acetylcholine receptor on ion flux activation and inactivation kinetics. *Biochemistry* **23:**2329–2338

Yee, A.S., Corley, D.E., McNamee, M.G. 1986. Thiol-group modification of *Torpedo californica* acetylcholine receptor: subunit localization and effects on function. *Biochemistry* **25:**2110–2119

Zanello, L.P., Aztiria, E., Antollini, S., Barrantes, F.J. 1996. Nicotinic acetylcholine receptor channels are influenced by the physical state of their membrane environment. *Biophys. J.* **70:**2155–2164